Electrochimica Acta 135 (2014) 404–411

Contents lists available at ScienceDirect

Electrochimica Acta

journal homepage: www.elsevier.com/locate/electacta

Electrochemical behaviour of different redox probes on single wall carbon nanotube buckypaper-modified electrodes

J.M. Sieben [a], A. Ansón-Casaos [b], F. Montilla [c], M.T. Martínez [b], E. Morallón [c,*]

[a] Instituto de Ingeniería Electroquímica y Corrosión (INIEC), Universidad Nacional del Sur, Av. Alem 1253 - Bahía Blanca (B8000CPB)- Buenos Aires–Argentina
[b] Instituto de Carboquímica, CSIC, Miguel Luesma 4, 50018 Zaragoza, Spain
[c] Departamento de Química Física and Instituto Universitario de Materiales, Universidad de Alicante, Ap. 99 Alicante, Spain

ARTICLE INFO

Article history:
Received 28 November 2013
Received in revised form 28 April 2014
Accepted 4 May 2014
Available online 10 May 2014

Keywords:
single-walled carbon nanotubes
buckypaper
electrochemical properties
redox probes

ABSTRACT

In the present work, the electrochemical properties of single-walled carbon nanotube buckypapers (BPs) were examined in terms of carbon nanotubes nature and preparation conditions. The performance of the different free-standing single wall carbon nanotube sheets was evaluated via cyclic voltammetry of several redox probes in aqueous electrolyte. Significant differences are observed in the electron transfer kinetics of the buckypaper-modified electrodes for both the outer- and inner-sphere redox systems. These differences can be ascribed to the nature of the carbon nanotubes (nanotube diameter, chirality and aspect ratio), surface oxidation degree and type of functionalities. In the case of dopamine, ferrocene/ferrocenium, and quinone/hydroquinone redox systems the voltammetric response should be thought as a complex contribution of different tips and sidewall domains which act as mediators for the electron transfer between the adsorbate species and the molecules in solution. In the other redox systems only nanotube ends are active sites for the electron transfer. It is also interesting to point out that a higher electroactive surface area not always lead to an improvement in the electron transfer rate of various redox systems.

In addition, the current densities produced by the redox reactions studied here are high enough to ensure a proper electrochemical signal, which enables the use of BPs in sensing devices.

1. Introduction

Since their discovery in the early 90's by Iijima [1], carbon nanotubes (CNTs) has stimulated intense research in nanoscience due to their high electronic conductivity and superior mechanical performance, high surface area, flexibility, high aspect ratio and also excellent chemical stability [2,3].

The preparation of SWCNT-based films has been up to date the most successful way to transfer SWCNTs properties from the nano- to the microscale level [4], leading to formation of strong and lightweight materials [5]. As a result, buckypapers (BPs) and SWCNT films can be considered as very promising materials for transistors in flexible electronics sensors, transparent electrodes in solar cells, displays, artificial actuators and nanostructured electrodes in batteries, supercapacitors and fuel cells [6].

In recent years CNTs have acquired a very important role in electroanalytical chemistry principally due to their capability for mediate electron-transfer reactions in solution and to their great electroactive surface area that guarantee excellent electrode sensitivity [7–10]. Therefore, BPs-based electrodes can be used in the development of new types of electrochemical sensors and biosensors.

The origin of the electrochemical activity of CNTs has been suggested to be the result of the electron transfer from the open ends of the tubes (edge-plane-like defects) [11,12]. However, defects can also occur in the walls (basal-plane-like sites) due to the helicity and low dimensionality of the nanotubes [13]. In addition the presence of oxygenated moieties is expected to have an important effect on electrochemical behavior. As a consequence, carbon nanotubes of diverse nature yield different rate constants due to structure-dependent variations in the local density of states (DOS) at the Fermi level [13,14]. In this context, the electrochemical properties of buckypapers can be evaluated by using different redox systems as benchmarks for the identification of carbon electroactive sites [15]. A complete classification of redox probes according

* Corresponding author.
E-mail address: morallon@ua.es (E. Morallón).

http://dx.doi.org/10.1016/j.electacta.2014.05.016
0013-4686/

to their kinetic sensitivity to particular surface sites on carbon electrodes was reported by McCreery [16]. For example, the ferrocene/ferrocenium and $Ru(NH_3)_6^{3+/2+}$ couples are considered as outer-sphere redox systems and their electrochemical behavior depends only on the electronic structure of the electrode (DOS at the Fermi level). They are insensitive to the presence of an adsorbed monolayer film and the nature of the carbon electrode surface. On the contrary, there are redox systems such as $Fe(CN)_6^{3-/4-}$, ascorbic acid and dopamine that are influenced by the existence of defects on the electrode surface. In addition, there are also some redox probes that depend strongly on the presence of surface oxides such as $Fe(H_2O)_6^{3+/2+}$.

The main objective pursued in the present investigation is to analyze how the electrochemical behavior of SWCNTs-based buckypapers depend on the nature of the carbon nanotubes, oxidation degree and preparation conditions. A systematic and complete analysis of the electrochemical properties of the different BPs has been performed on the basis of voltammetric studies with six redox systems in aqueous electrolyte. This study is expected to provide basic but useful information for the design, construction and optimization of a new type of flexible electrochemical sensor.

2. Experimental

SWCNTs were purchased from Carbon Solutions Inc. (AP-SWNT grade) and from Sigma-Aldrich (704121, SWeNT SG 76 grade). SWCNTs from Carbon Solutions (CS-SWCNTs) are synthesized by the electric arc reactor method using Ni/Y catalyst and contain ~30 wt% metal residue. The average diameter and length of the CS-SWCNTs is 1.5-1.6 nm and 509 nm, according to AFM measurements [17]. Sigma-Aldrich nanotubes (SW-SWCNTs) are synthesized by a chemical vapor deposition method using cobalt and molybdenum as the catalysts (CoMoCAT process). According to the provider, SW-SWCNTs have diameters of 0.7-1.1 nm and an average length of 800 nm. Metal residue is less than 10 wt% and more than 50% of the nanotubes show (7,6) chirality.

Three carbon nanotube buckypapers (BP1, BP2 and BP3) were prepared by vacuum filtration through 0.1 μm Omnipore membranes (Millipore). BP1 was made of pristine CS-SWCNTs, while BP2 contained oxidized nanotubes (Ox-CS-SWCNTs). Oxidation of the CS-SWCNTs was performed by thermal treatment in air atmosphere in an oven at 350 °C for 1 h. The weight change during the process was from 70 to 64 mg (8.6% weight loss). BP3 was made of pristine SW-SWCNTs.

For BP1, 30 mg of the CS-SWCNT powder was tip sonicated (Hielscher DRH-UP400S ultrasound tip, with 3 mm tip diameter, 400 W maximum power and 24 kHz maximum frequency) at 60% amplitude, in continuous regime in 25 ml of dimethyl-formamide (DMF), filtered and washed with ether. For BP2 30 mg of Ox-CS-SWCNTs were tip sonicated in 25 ml of N-methyl-pyrrolidone (NMP). For BP3, 30 mg of SW-SWCNTs were tip sonicated in 25 ml of NMP. Curiously, BP3 experienced radial shrinkage after filtration, during the drying of the residual NMP.

Buckypapers sheets (~5 mg cm^{-2}) were stuck onto polished glassy carbon (GC) discs of 0.07 cm^2 exposed geometric area by using a diluted Nafion solution (5 wt%.).

Sulphuric acid, sodium hydroxide, dipotassium hydrogen phosphate, potassium dihydrogen phosphate, potassium hexacyanoferrate(II) trihydrate, potassium hexacyanoferrate(III), iron(II) sulphate heptahydrate and iron(III) sulphate hydrate were provided by Merck (p.a.) without further purification. Besides, ferrocenium hexafluorophosphate ($FcPF_6$), l-ascorbic acid (AA), dopamine (DA), p-benzoquinone (Q) and hydroquinone (HQ) were also used as received (Sigma-Aldrich, p.a.). All solutions were prepared with purified water ($\rho \approx 18.2$ MΩ cm) obtained from an Elga Labwater Purelab system. The concentration of redox probes for the determination of the electrochemical behaviour of the buckypapers-modified electrodes were as follows: 1.0×10^{-2} mol dm^{-3} $K_3Fe(CN)_6$/1.0×10^{-2} mol dm^{-3} $K_4Fe(CN)_6$, 1.0×10^{-2} mol dm^{-3} $FeSO_4$/1.0×10^{-2} mol dm^{-3} $Fe_2(SO_4)_3$, 5×10^{-4} mol dm^{-3} $FcPF_6$, 1.0×10^{-2} mol dm^{-3} ascorbic acid, 1.0×10^{-3} mol dm^{-3} mM dopamine, 1.0×10^{-3} mol dm^{-3} p-benzoquinone/1.0×10^{-3} mol dm^{-3} hydroquinone. Phosphate buffer solution (PBS, pH = 7.0) was prepared by mixing 300 ml of a 0.25 mol dm^{-3} K_2HPO_4 solution with 200 ml 0.25 mol dm^{-3} KH_2PO_4.

Conventional three-compartment glass cells were used to run the electrochemical experiments at room temperature with a PAR 263 potentiostat/galvanostat. The counter-electrode was a platinum wire, and a reversible hydrogen electrode (RHE) immersed in the same electrolyte served as reference. All potentials mentioned in this work are referred to this electrode. All solutions were thoroughly deaerated by bubbling N_2 gas for 30 min. After bubbling, an inert nitrogen atmosphere was maintained over the electrolyte during the experiments. Cyclic voltammograms were performed at different scan rates, ranging from 10 to 500 mV s^{-1}. The current density was calculated from the geometric area of the electrode. All experiments were performed in triplicate to ensure reproducibility.

Characterization of the SWCNT powder samples was performed by visible/near infrared (Vis/NIR) absorption spectroscopy and thermogravimetric analysis (TGA) as previously reported [18]. Elemental oxygen was determined using a Thermo Flash 1112 analyzer. Samples were heated to 1080° C, and the pyrolysis products were reduced to CO in a carbon black bed and analyzed by gas chromatography. Surface chemistry characterization of the SWCNT powders was accomplished by Fourier-transform infrared (FTIR) spectroscopy measured in a Bruker Vertex 70 spectrometer. For IR measurements, less than 0.5 mg of the samples were mixed with spectroscopic KBr (200 mg) in an agate mortar and pressed (10 Tm, 2 min) to form pellets (ϕ = 13 mm). The pellets were dried at 85 °C for 3 days.The morphology of the buckypapers architecture was analyzed using a SEM microscope (Hitachi S3000 N).

3. Results and Discussion

3.1. Characterization of single-walled carbon nanotubes and buckypapers

The characterization by Vis/NIR spectroscopy of the pristine and oxidized SWCNT has been previously published [18,19]. CS-SWCNT spectrum shows the characteristic bands of metallic (M_{11} band) and semiconducting (S_{22} band) SWCNTs at approximately 600-800 nm and 900-1200 nm, respectively. The Ox-SWCNT Vis-NIR spectrum profile is almost identical to that for pristine CS-SWCNTs, only a small difference in the M_{11} and S_{22} band intensity is observed. Consequently, no substantial changes in the chirality and diameter distribution took place during the oxidative thermal treatment of the SWCNT. CS-SWCNTs were produced by the arc discharge method and are highly graphitized, while SW-SWCNTs were produced by chemical vapor deposition at a relatively low temperature and may contain a substantial amount of structural defects.

The Vis-NIR spectrum of SW-SWCNTs is clearly different from that of CS-SWCNTs. The intensity of the SW-SWCNTs absorption bands is high indicating a remarkably pure SWCNT material. The Vis-NIR spectrum of BP3 sample shows a prominent band corresponding to the (7,6) chirality in agreement with the provider specifications [18].

The oxygen content of the samples (2.6 wt.% CS-SWCNTs, 5.1 wt.% SW-SWCNts, 10.8 wt.% Ox-CS-SWCNTs) indicates that the pristine SWCNTs contain some oxygenated functional groups introduced during the synthesis process. After oxidation, the

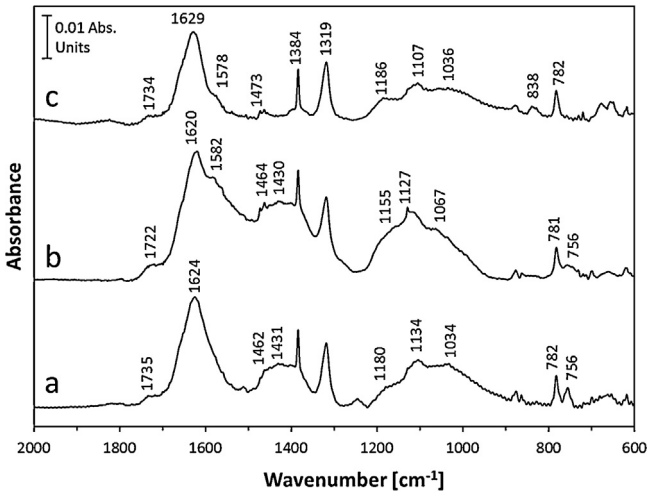

Figure 1. Baseline subtracted FTIR spectra for various SWCNT powder materials: a) CS-SWCNT from Carbon Solutions Inc, b) CS-SWCNT after a treatment at 350 °C in static air (Ox-CS-SWCNT), and c) SW-SWCNT from Sigma-Aldrich 704121 (SWeNT SG 76).

oxygen content of the CS- SWCNTs increases considerably. Fig. 1 shows FTIR spectra from 600 to 2000 cm-1 of the SWCNTs used in the buckypapers preparation. All spectra present the 1580cm^{-1} band corresponding to the aromatic C=C structural vibrations and a broad band between 1050 and 1300cm^{-1} (C-O stretching from ethers, alcohols, anhydrides, lactones). No substantial changes were observed in the IR spectrum profile after the thermal oxidation of CS-SWCNTs in air atmosphere. However, all bands related to C-O oxygen groups increase their intensity in the 1050–1300cm^{-1} region. The oxidized sample also shows increased intensity in the 1580 cm^{-1} region that could corresponds to C=O bonds probably quinones (1550–1600cm^{-1}). Gas phase oxidation of carbon materials mainly increases the concentration of hydroxyl and carbonyl surface groups [20]. IR spectrum of SW-SWCNTs, shows a shoulder at 1578 cm-^{1} that is not visible in pristine CS-SWCNTs. The spectrum shows very low intensity in the 1400-1500 cm-^{1} region, contrarily to what is seen in both as grown and oxidized CS-SWCNTs, these bands could corresponds to more stable oxygenated functional groups that evolve at higher temperatures as seen in the thermogravimetric analysis of these samples [18].

Fig. 2 provides the comparison of the voltammetric response obtained at bare GC and buckypaper-modified GC electrodes in 0.5 mol dm^{-3} H_2SO_4 solution at a scan rate of 50 mV s^{-1}. The

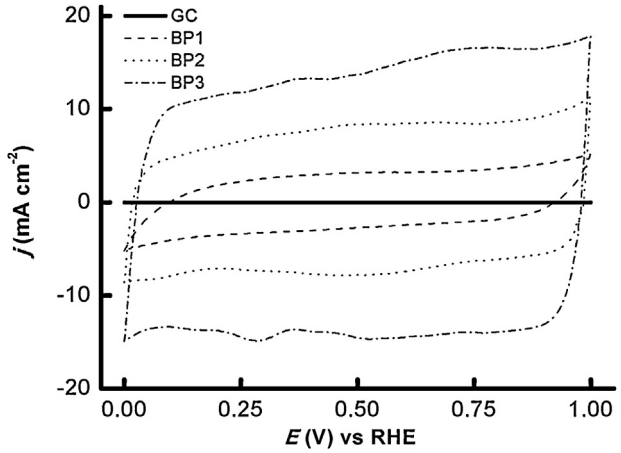

Figure 2. Steady cyclic voltammograms of all carbon nanotube buckypapers-supported GC electrodes in 0.5 M H_2SO_4. υ = 50 mV s^{-1}.

Table 1
Electrochemical parameters extracted from CV measurements at 50 mV s^{-1} in 0.5 M H_2SO_4 electrolyte solution.

Material	[1]S/cm^2	[2]S_w/m^2 g^{-1}	C/F g^{-1}
BP1	468	149	15
BP2	1019	357	36
BP3	1899	365	37

[1] Electroactive surface area. [2] Specific surface area.

voltammograms show a current increase for all the BPs electrodes and reveal the quasi-rectangular shape characteristic of a double layer profile with non-faradaic processes, indicating that the main contribution to capacitance is the charge and discharge of the double layer. In addition, the electrodes BP2 and BP3 that correspond to SWCNTs with higher oxygen content, exhibit two pairs of redox peaks that are characteristic of the presence of oxygenated surface groups such as alcohols, carboxylic acids and quinones [21–23], mostly located at the open end of the nanotubes. These terminal atoms influence the electrochemical interfacial state of the carbon surface and its electrochemical double-layer properties [24].

The specific surface area (S_w) and the electroactive surface area (S) of all materials can be estimated assuming a value of 10 μF cm^{-2} for the specific capacitance of CNTs [25]. The information for all buckypapers has been listed in Table 1. The gravimetric capacitance is lower than that informed for pristine single walled carbon nanotubes (52 F g^{-1}) [26], but very similar to those reported for electrodes prepared by drop casting, air brushing, electrospraying and SWCNTs mixed with cellulose filter paper (35-42 F g^{-1}) [27,28].

The difference in the magnitude of the gravimetric capacitance can be explained by the difference in packing density of the carbon nanotubes bundles. On the other hand, the different solvents, interact in different way with pristine and oxidized SWCNTs and influence the degree of dispersion previous to de buckypapers formation and as a consequence, influence the electroactive area in the electrode. On the other hand, the presence of carbon-oxygen moieties has an important effect on the electrochemical properties of BP2 and BP3.

Fig. 3 shows the SEM images of the surface morphology of the BP-modified GC electrodes. As illustrated, there are some differences in surface morphology of all CNTs films. For the BP1 electrode a disordered tangle of nanotube bundles is shown at the surface. BP2 exhibits a porous and rough surface due to the presence of entangled mats of SWCNTs, whereas BP3 exhibits a more open surface structure and the nanotube bundles are thickly interwoven forming ropes.

3.2. *Electrochemical properties of carbon buckypapers*

Once verified the electrochemical performance and the microscopic characteristics of the three buckypapers, it is very important to evaluate their electrochemical behaviour to electron transfer processes at the electrode/electrolyte interface. In order to compare the electrochemical properties of the different buckypapers with several redox probes the electron transfer rate constant (k^0) from the peak separation by using the Nicholson method [29] and the numerical approach developed by Mahé et al. [30] have been determined.

The determination of k^0 values were made with the diffusion coefficients obtained from Ref. [31].

The standard electrochemical rate constant (k^0) can be calculated from the cyclic voltammetric experiments by assuming values of the cathodic and anodic charge transfer coefficients α = 0.5 and

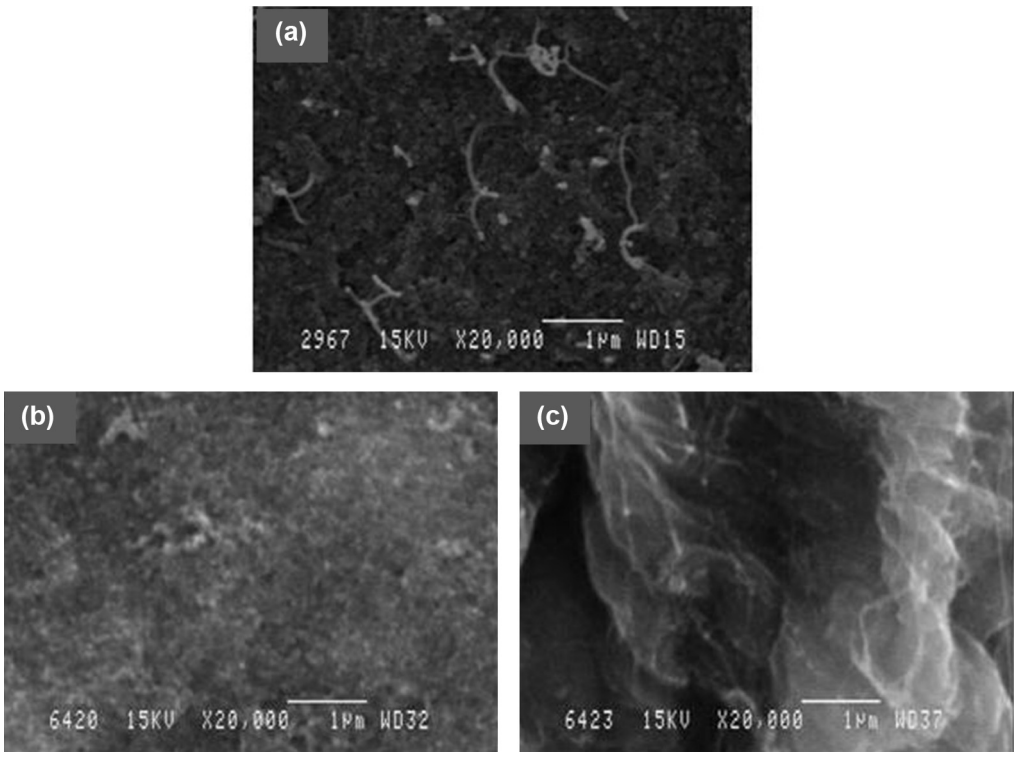

Figure 3. SEM images of the SWCNT buckypapers: (a) BP1, (b) BP2, (c) BP3.

equal diffusion coefficients for the oxidized and reduced species (D):

$$k^0 = \sqrt{\left(\frac{\pi DnF\nu}{RT}\right)}\psi \quad (1)$$

Here, n, F, R and T have their usual significance, while ψ is a dimensionless charge transfer parameter that depends on the peak separation and ν is the scan rate of the cyclic voltammetry experiments.

In addition, the scan rate dependence with the peak heights for the anodic and cathodic curves was evaluated by the Randles-Ševčik equation:

$$I_p = 2.687 \times 10^5 An^{3/2}(D\nu)^{1/2}C \quad (2)$$

Here, I_p, is the peak current (A), A is the electroactive area (cm^2), C is the concentration of the electroactive specie (mol cm^{-3}), n is the number of exchanged electrons, D is the diffusion coefficient (cm^2 s^{-1}) and v is the scan rate (V s^{-1}), respectively. From these plots it was observed that for each electrode and every redox probe the peak current varies linearly with the square root of the scan rate (some selected plots are shown in Fig. SI1), so the buckypaper modified electrodes mimics the characteristics of a solid planar macroelectrode. That is, the diffusion layers originated at the disordered nanotubes bundles are overlapped, which in turns results in a semi-infinite planar diffusion controlled process [31].

Despite ferrocene solubility is very limited in water, the $Fc^{+/0}$ couple has been frequently used as a standard surface insensitive reference redox probe to characterize the electrochemical properties of carbon electrodes in aqueous electrolytes [32–34]. In aqueous solutions, ferrocene oxidation involves a single-electron transfer mechanism preceded by a weak adsorption process, which depends on the electronic structure of the electrode.

Fig. 4a provides the voltammetric response of the bare GC electrode and the buckypapers modified electrodes at 50 mV s^{-1}. BP1 electrode exhibits a higher background pseudocapacitive current with a peak separation of 145 mV, while the oxidation peak is shifted to more positive potentials with respect to the bare GC electrode (1.05 V). The redox peaks are hardly detected in the free-standing Ox-CS-SWCNT sheet (BP2) due to the high pseudocapacitance from the oxygen-containing groups, but similar positive shift of the anodic peak with respect to GC were observed. On the other hand, the redox peaks are clearly visible in the CV curve of BP3, even though the charge of the double layer region is about two times higher than that of BP1. The oxidation peak appears at 1.16 V while the complementary cathodic peak emerges at about 0.87 V. The peak separation values at the last two electrodes were found to be between 254 and 285 mV. It is worth nothing that the highest degree of reversibility was obtained with BP1, which have quite low content of oxygenated functionalities on the nanotubes surface. On the contrary, the buckypapers electrodes with higher percentage of oxygenated moieties (BP2 and BP3) exhibited a significant decrease in the reversibility of the one-electron process. This behavior can be explained in terms of the stronger adsorption of ferrocene on these two electrodes.

The ferro/ferricyanide couple, which is classified as "surface-sensitive" but not as an "oxide-sensitive" redox probe, has been employed as a benchmark for comparing different carbon electrodes. It is believed that the ability of CNTs to facilitate this reaction is consequence of the high reactivity of the tips (*i.e.*, the edge-plane like sites [12]), although the defects in the walls may play an important role in the electrochemical behavior of nanotube-based electrodes [16]. Figure 4b depicts the voltammetric behavior of $Fe(CN)_6^{3-/4-}$ redox couple in a buffered phosphate solution. The peak potential separation of GC is 440 mV. In the BP1 and BP2 electrodes the anodic peak and the cathodic counterpart appear at more positive potentials and the voltammetric profiles exhibit a pair of adsorption pre-peaks. According to the simulations by Wopschall et al. [35], the shift of the oxidation peak to a more positive potential value and the appearance of a pre-peak are due to an electrode reaction that involves the strong adsorption of the product. Although being a rather unexpected behavior, it has also

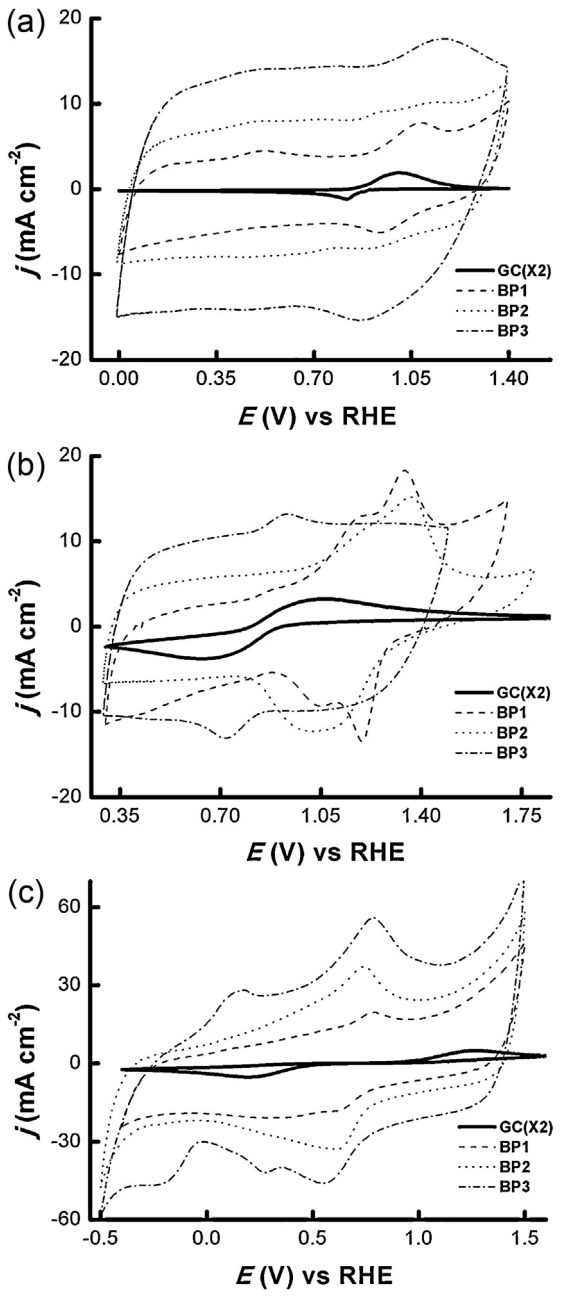

Figure 4. Steady voltammograms of the electrodes in (a) 1 mM FcPF6 + pH 7.0 PBS solution, (b) 10 mM $K_3Fe(CN)_6$/10 mM $K_4Fe(CN)_6$ + pH 7.0 PBS solution and (c) 10 mM $FeSO_4$/10 mM $Fe_2(SO_4)_3$ + 0.5 M H_2SO_4 solution. Scan rate was 50 mV s^{-1}. Note the current for GC have been multiplied by a factor of 2 (as indicated in parentheses).

been recently reported for imidazolium-based polymer/MWNT-modified GC electrodes [36]. Here, the peak that appears at ~1.3 V can be associated with the electron transfer of solution-phased $Fe(CN)_6^{3-/4-}$ at the electrode, while the pre-peak can be attributed to the electrochemical process of $Fe(CN)_6^{3-/4-}$ adsorbed onto the electrode surface. For the BP1 electrode the peak separation at 50 mV s^{-1} is 145 mV, with the anodic peak centered at 1.34 V and the cathodic one centered at 1.19 V. In comparison, the oxidized sample (BP2) has peak separation of 249 mV, with the oxidation peak centered at about 1.36 V and the cathodic counterpart at ~1.12 V. The difference in electron transfer rates between these two buckypaper-modified electrodes can be explained as result

Table 2
Voltammetric peak separation (ΔE_p) at 50 mV s^{-1} and heterogeneous rate constant (k^0), for a series of redox reaction performed with mirror polished GC and buckypaper-modified electrodes.

Electrode	Redox probe	ΔE_p mV	k^0 cm s^{-1}
GC	$Fc^{+/0}$	170	1.07×10^{-3}
BP1		145	1.54×10^{-3}
BP2		254	3.58×10^{-4}
BP3		285	3.53×10^{-4}
GC	$Fe(CN)_6^{3-/4-}$	440	5.71×10^{-5}
BP1		145	1.47×10^{-3}
BP2		249	3.57×10^{-4}
BP3		202	1.64×10^{-4}
GC	$Fe^{2+/3+}$	1070	1.42×10^{-7}
BP1		125	2.21×10^{-3}
BP2		125	2.21×10^{-3}
BP3		235	5.30×10^{-4}
GC	Dopamine	330	9.39×10^{-6}
BP1	(DA)	140	4.74×10^{-4}
BP2		213	2.00×10^{-4}
BP3		201	2.25×10^{-4}
GC	Ascorbic Acid	810	-
BP1	(AA)	570	-
BP2		625	-
BP3		721	-
GC	Quinone/	496	5.00×10^{-5}
BP1	Hydroquinone	160	3.96×10^{-4}
BP2	(Q/HQ)	100	1.07×10^{-3}
BP3		358	1.88×10^{-4}

of a slightly higher amount of exposed edge-plane defects to the electrolyte solution.

Interestingly, the shape of the CV obtained with BP3 is different to that recorded for the other electrodes. The peak separation is slightly lower than those of BP2, and the position of the redox waves is very different. The oxidation peak appears at ~0.92 V during the forward scan and the corresponding reduction peak appears at ~0.72 V during the backward scan. In this case, it seems possible that the redox process takes place in the absence of $Fe(CN)_6^{3-/4-}$ adsorbed species. Therefore, this difference in behavior may be associated with the high percentage of (7,6) chiral type carbon nanotubes in this sample. It is well known that the density of states (DOS) has a strong dependence on nanotube diameter, chirality, and type of carbon nanotubes [37,38]. Recent reports have showed a chirality dependence on the binding strength of different adsorbed species on the nanotubes surface [39–41].

The effect in k^0 derived from the presence of the buckypapers in the electrode surface is expected to become more visible for the aqueous $Fe^{2+/3+}$ redox test reaction. This is because the $Fe(H_2O)_6^{3+/2+}$ redox system depends strongly on the presence of oxygen moieties at defect sites on carbon electrodes [42,43]. As depicted in Fig. 4c, the presence of the buckypapers enhances noticeably the reversibility of the redox process with respect to the bare GC electrode. The oxidation peak appears at more negative potentials, while the corresponding reduction peak appears at more positive potentials during the reverse scan. For this redox reaction the heterogeneous electron transfer constants increase by 3 or 4 orders of magnitude (Table 2). From the comparison of the voltammetric profiles of all buckypaper-modified electrodes, it can be seen that BP1 and BP2 has smaller peak separation than BP3. Meanwhile, the BP3 electrode has peak separation of 235 mV. According to the results, the difference in electron transfer kinetic observed for this redox probe can be attributed to two causes. The first one related to the amount of available edge-plane defects, which is direct consequence of the preparation method, and the second one linked to the oxygen-containing surface functional group coverage (i.e., the surface O/C ratio). Apart from that, the voltammetric curve of BP3 exhibits a pair of adsorption pre-peaks and the oxidation wave appears at more positive potentials indicating the $Fe(H_2O)_6^{3+}$

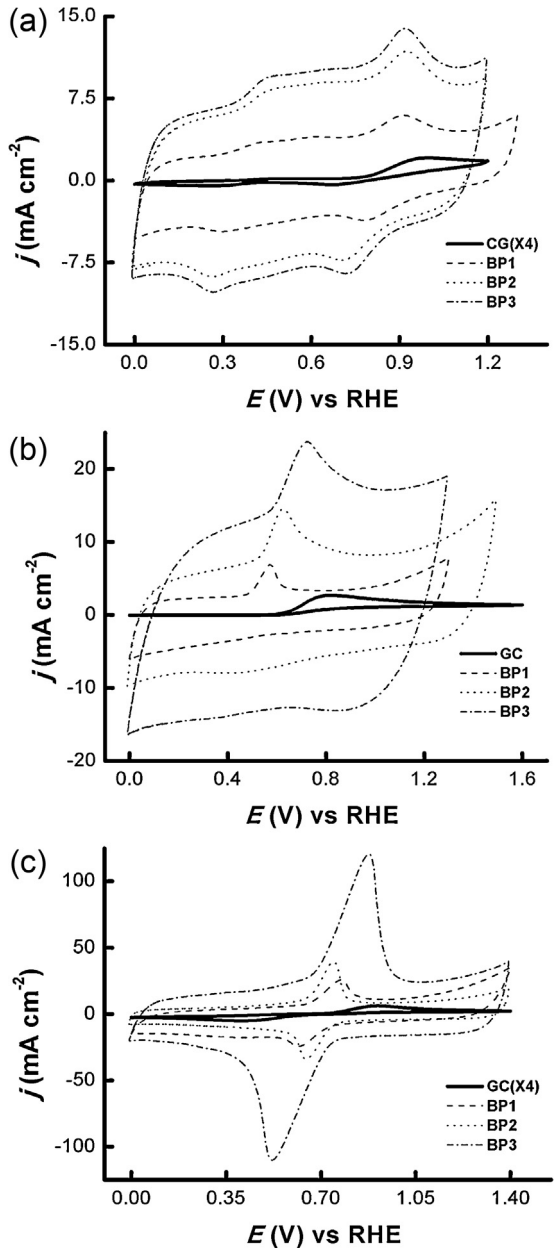

Figure 5. Steady voltammograms of the electrodes in (a) 1 mM dopamine + pH 7.0 PBS solution, (b) 10 mM ascorbic acid + pH 7.0 PBS solution and (c) 1 mM p-benzoquinone/1 mM hydroquinone + 0.5 M H_2SO_4 solution. Scan rate was 50 mV s^{-1}. Note the current for GC has been multiplied by a factor of 2 (as indicated in parentheses).

is strongly adsorbed onto the electrode surface. The difference in behavior is likely caused by the nature of this type of SWCNTs as determined by UV/Vis spectroscopy and by the presence of different oxygenated moieties on the surface of BP3, as evidenced by FTIR and TGA analysis of the carbon nanotubes samples [19].

In order to gain more knowledge on the electron transfer characteristics of the buckypapers, some organic redox systems with biological importance were tested and the results presented in Fig. 5. The electrochemical behavior of dopamine, a catecholamine excitatory chemical neurotransmitter extensively examined in electrocatalysis, is depicted in Fig. 5a. The electro-oxidation of dopamine has been observed to be fast on hydrogen-terminated atoms and on step edge defects [44,45]. Dopamine is oxidized in a two-step process that involves the transference of two electrons and two protons preceded by a strong adsorption step. The first oxidation peak observed in the voltammograms at ~0.45 V and the corresponding reduction peak at about 0.3 V are associated with the dopaminechrome redox transitions. While the second oxidation peak located at about 0.88 V and the reduction peak at ~0.73 V are related to the dopamine-dopaminequinone redox couple [15]. The k^0 values for the dopamine couple at the buckypaper-modified electrodes are two orders of magnitude higher than at the bare GC electrode. For the buckypapers with low oxygen content BP1, the peak separation is 140 mV. In comparison, the electrodes BP2 and BP3, with 5-10 wt%. Oxygen content, have peak separations of 213 and 201 mV, respectively. Since the electrons transfer kinetic has been established to be independent of the oxygen-containing functional groups, the previous result could indicate that the number of preferential sites that participates in the electrochemical mechanism of the dopamine redox reaction is higher on BP1 than on BP2 and BP3.

Ascorbic acid is another essential biomolecule that participates in a large number of metabolic reactions. As depicted in Fig. 5b, the electrochemical behavior of AA is characterized by the appearance of a single oxidation peak in the potential region between ca. 0.6 V and 0.8 V, which corresponds to the irreversible change of Vitamin C in dehydroascorbic acid via a multistep process that involves the transfer of two electrons and one or two protons, depending on the pH [46]. Results from literature indicated that this redox reaction is not sensitive to surface oxides, but it is inhibited by the adsorption of a monolayer, suggesting that the redox reaction depends on a surface interaction between the redox center and some sites on the carbon support surface [43]. As noted in Table 2, the buckypapers enhance the electrochemical parameters of the reaction with greater or lesser success depending on the amount of defective sites in each material, which is related to either the degree of surface oxidation, or the effect of the preparation method and nanotubes nature. As it was already demonstrated for the $Fe(CN)_6^{3-/4-}$ redox reaction, the BP1 electrode has the fastest electrons transfer rate.

The quinone-based couples perform crucial biological functions as electron-proton transfer mediators in the oxidative phosphorylation of ADP to ATP, or photosynthesis and respiration processes [47–49]. The electrochemical response of Q/HQ on the surface of the electrodes in an unbuffered aqueous acid media is shown in Fig. 5c. The voltammetric profiles show a pair of redox waves centered at about 0.7 V, which are associated with the transfer of two electrons and two protons, according to the "scheme of squares", through a self-catalytic quinone layer that is adsorbed (physisorbed or chemisorbed) on the electrode surface [46,50]. It can be seen from Table 2 that k^0 increases one or two order of magnitude for the buckypaper-modified electrodes with respect to the bare GC electrode. The oxidation and reduction peaks for BP1 and BP2 can be observed at about 0.76 ± 0.02 V and 0.62 ± 0.02 V, respectively. For BP1 the peak separation is 160 mV. It is noteworthy that this value is very similar to those reported for dopamine oxidation, although the oxidation and reduction peaks appear at less positive potentials. This behavior is similar to that reported by Duvall and McCreery [44] on polished and modified surfaces of GC electrodes. In comparison the electrode BP2 has ΔE_p value of 100 mV. This behavior seems to be very unusual, considering that changes in surface oxide coverage has little influence on hydroquinone/benzoquinone kinetics [44,46]. However, such observation is consistent with a redox reaction in which the lactone-like moieties on the surface of the Ox-CS-SWCNT mediate electron transference via a proton-coupled mechanism, as is the case with activated GC electrodes [50,51], thus accelerating the redox process.

On the other hand, significant larger value of peak separation is reported for BP3 electrode. For this electrode the anodic peak appears at about 0.88 V during the forward scan and the corresponding cathodic peak appears at 0.65 V during the reverse scan, while the bare GC electrode exhibits irreversible

Table 3
Oxidation peak current density obtained at 50 mVs^{-1} normalized with the BP's mass, electroactive area for electron transfer obtained from Randles-Ševčik equation and percentage of electroactive sites for the electrochemical reaction of the different redox probes for buckypaper electrodes.

Electrode	Redox probe	j_p mA mg^{-1}	A cm^{-2}	Active sites %
BP1	$Fe(CN)_6^{3-/4-}$	4.06	0.84	0.18
	$Fe^{2+/3+}$	4.35	0.85	0.18
	$Fc^{+/0}$	1.15	2.34	0.50
	DA	1.32	1.00	0.21
	AA	1.53	0.12	0.03
	Q/HQ	5.75	3.92	0.84
BP2	$Fe(CN)_6^{3-/4-}$	3.72	0.69	0.07
	$Fe^{2+/3+}$	9.13	1.62	0.16
	$Fc^{+/0}$	2.49	4.61	0.45
	DA	2.89	1.98	0.19
	AA	3.57	0.26	0.03
	Q/HQ	9.63	5.99	0.59
BP3	$Fe(CN)_6^{3-/4-}$	1.77	0.60	0.03
	$Fe^{2+/3+}$	7.51	2.43	0.13
	$Fc^{+/0}$	2.37	7.99	0.42
	DA	1.86	2.33	0.12
	AA	1.38	0.18	0.01
	Q/HQ	16.19	18.37	0.97

oxidation/reduction peaks at ~0.91 V and ~0.41 V, respectively. As noted previously, the electrochemical behavior of BP1 can be associated with the very low amount of edge-plane like sites exposed to the electrolytic solution. In the case of BP3, the different nature of these SWCNTs and some kind of oxygenated functional groups could lead to electrostatic repulsion between the surface and the Q/HQ couple at pH 1 or to the incomplete surface coverage of Q/HQ [45].

In order to complete the information, we have estimated the electroactive surface area for each reaction (A) from the slope of the Randles-Ševčik plots and the percentage of actives sites (surface area that effectively transfers the charge to the species in solution) from the ratio between A and S [15]. As shown in Table 3, for all buckypaper-based electrodes the percentage of active sites is higher for the ferrocene/ferrocenium and quinone/hydroquinone couples. However, the number of active sites for these redox reactions is less than 1%. For the other redox probes, the number of active sites is even lower than 0.25%, and for example reach values of around 0.18 and 0.01% for $Fe(CN)_6^{3-/4-}$ (or $Fe^{2+/3+}$) and AA respectively. This behavior can be attributed to the fact that the tips of the nanotubes, which have better electrochemical efficiency for electron transfer, represent only a small amount of the whole electrode surface. However, in the case of DA, Fc, and Q/HQ the voltammetric response should be thought as a complex contribution of different tips and sidewall domains which offer different surface energies and electrochemical behaviour [33,52], because the carbon nanotubes walls can also act as mediators for the electron transfer between the adsorbate species and the molecules in solution.

It is worthwhile to note that some general tendencies emerged from Table 3. First, the buckypaper composed by non-oxidized SWCNTs (BP1) present similar values of A for both $Fe(CN)_6^{3-/4-}$ and $Fe^{2+/3+}$ redox systems, suggesting that the tips of the nanotubes are strongly oxidized [15]. Second, for the $Fe^{2+/3+}$ redox system, the electroactive surface area increases for the Ox-SWCNTs papers (BP2 and BP3), indicating the presence of oxygenated moieties at the sidewall of the nanotubes. Finally, for the other redox benchmarks (Fc, DA, AA and Q/HQ), the electroactive surface area is higher for the Ox-SWCNT buckypapers than for the pristine electrode materials. However, it is interesting to note that a higher electroactive surface area not always lead to an improvement in the electron transfer rate, as in the case of AA, DA and Fc, probably due to the strong adsorption of these redox molecules on the electrode surface and to high oxidation degree of the sidewall defects created in pretreatments, amongst other issues.

As was commented previously, the difference between the buckypapers behavior can be associated with the nature of the carbon nanotubes (nanotube diameter, chirality, aspect ratio, etc.), oxidation degree and preparation conditions.

Finally, it can be mentioned that Table 3 also includes the peak current density normalized to the mass of the electrode material. For all the redox couples the anodic peak current density depends almost exclusively on the electroactive surface area of the buckypapers-modified electrode. The current densities produced by the redox reactions studied here are high enough to ensure a proper electrochemical signal, which enables the use of BPs-modified electrodes as transducers. However, the signal to background should be improved in order to detect small electrochemical signals. So, this issue will be the object of a further investigation.

4. Conclusions

In this study it has been shown how the electrochemical properties of different single-walled carbon nanotube buckypapers are influenced by the nature of the carbon nanotubes and preparation conditions. Several redox probes were employed to examine in detail the electrochemical behaviour of the different SWCNTs that make up the composites. The buckypaper-modified electrodes improve the redox transfer reaction with greater or lesser success, depending on the degree of surface oxidation, nanotubes nature and buckypapers porosity. The presence of the buckypapers enhances noticeably the reversibility of the $Fe(H_2O)_6^{3+/2+}$ redox process with respect to the bare GC electrode, reaching an increase of over 4 orders of magnitude in the heterogeneous electron transfer constant. Significant effects on the electron transfer rate are also observed for the three molecules that are of biological interest (dopamine, ascorbic acid and quinone).

For all buckypaper-based electrodes the percentage of active sites is maximum for the ferrocene/ferrocenium and quinone/hydroquinone couples, but even in these cases the values do not exceed 1%. For the other redox probes, the number of active sites is even lower. This behavior can be attributed to the fact that the tips of the nanotubes, which have better electrochemical behaviour for electron transfer, represent only a small amount of the whole electrode surface. On the contrary, for Fc and Q/HQ the electron transfer is also produced from the side-walls defects, because the carbon nanotubes walls can act as mediators for the electron transfer between the adsorbate species and the molecules in solution.

Acknowledgment

J.M.S. thanks Ministerio de Educación (SB2010-132). Financial support from MINECO (MAT2010-15273, TEC2010-15736 and PRIPIBAR-2011-1 projects),GV (PROMETEO2013/038 project) and and the Government of Aragon (DGA) and the European Social Fund (ESF) under Project DGA-ESF-T66 CNN is acknowledged.

References

[1] S. Iijima, Helical microtubules of graphitic carbon, Nature 354 (1991) 56.
[2] M. Valcarcel, S. Cardenas, B.M. Simonet, Role of carbon nanotubes in analytical science, Anal. Chem. 79 (2007) 4788.
[3] S. Iijima, T. Ichihashi, Single-shell carbon nanotubes of 1-nm diameter, Nature 363 (1993) 603.
[4] A. Ansón-Casaos, J.M. González-Domínguez, E. Terrado, M.T. Martínez, Surfactant-free assembling of functionalized single-walled carbon nanotube buckypapers, Carbon 48 (2010) 1480.
[5] M. Endo, H. Muramatsu, T. Hayashi, Y.A. Kim, M. Terrones, M.S. Dresselhaus, Buckypaper from coaxial nanotubes, Nature 433 (2005) 476.

[6] L. Hu, D.S. Hecht, G. Grüner, Carbon Nanotube Thin Films: Fabrication, Properties, and Applications, Chem. Rev. 110 (2010) 5790.
[7] M. Pacios, M. del Valle, J. Bartroli, M.J. Esplandiu, Electrochemical behavior of rigid carbon nanotube composite electrodes, J. Electroanal. Chem. 619–620 (2008) 117.
[8] P.J. Britto, K.S.V. Santhanam, A. Rubio, J.A. Alonso, P.M. Ajayan, Improved charge transfer at carbon nanotube electrodes, Adv. Mater. 11 (1999) 154.
[9] P.J. Britto, K.S.V. Santhanam, P.M. Ajayan, Carbon nanotube electrode for oxidation of dopamine, Bioelectrochem. Bioenerg. 41 (1996) 121.
[10] L. Agüí, P. Yáñez-Sedeno, J.M. Pingarrón, Role of carbon nanotubes in electroanalytical chemistry - A review, Anal. Chim. Acta 622 (2008) 11.
[11] C.E. Banks, R.R. Moore, T.J. Davies, R.G. Compton, Investigation of modified basal plane pyrolytic graphite electrodes: definitive evidence for the electrocatalytic properties of the ends of carbon nanotubes, Chem. Commun. 16 (2004) 1804.
[12] C.E. Banks, T.J. Davies, G.G. Wildgoose, R.G. Compton, Electrocatalysis at graphite and carbon nanotube modified electrodes: edge-plane sites and tube ends are the reactive sites, Chem. Commun. 7 (2005) 829.
[13] J.M. Nugent, K.S.V. Santhanam, A. Rubio, P.M. Ajayan, Fast electron transfer kinetics on multiwalled carbon nanotube microbundle electrodes, Nano Lett. 1 (2001) 87.
[14] I. Heller, J. Kong, K.A. Williams, C. Dekker, S.G. Lemay, Electrochemistry at single-walled carbon nanotubes: The role of band structure and quantum capacitance, J. Am. Chem. Soc. 128 (2006) 7353.
[15] D. Salinas-Torres, F. Huerta, F. Montilla, E. Morallón, Study on electroactive and electrocatalytic surfaces of single walled carbon nanotube-modified electrodes, Electrochim. Acta 56 (2011) 2464.
[16] R.L. McCreery, Advanced carbon electrode materials for molecular electrochemistry, Chem. Rev. 108 (2008) 2646.
[17] A.J. Blanch, C.E. Lenehan, J.S. Quinton, Parametric analysis of sonication and centrifugation variables for dispersion of single walled carbon nanotubes in aqueous solutions of sodium dodecylbenzene sulfonate, Carbon 49 (2011) 5213.
[18] J.M. Sieben, A. Ansón-Casaos, M.T. Martínez, E. Morallón, Single-walled carbon nanotube buckypapers as electrocatalyst supports for methanol oxidation, J. Power Sources 242 (2013) 7.
[19] A. Ansón-Casaos, M. Gonzalez, J.M. Gonzalez-Dominguez, M.T. Martinez, Influence of air oxidation on the surfactant-assisted purification of single-walled carbon nanotubes, Langmuir 27 (2011) 7192–7198.
[20] J.L. Figueiredo, M.F.R. Pereira, The role of surface chemistry in catalysis with carbons, Catal. Today 150 (2010) 2.
[21] J. Maruyama, I. Abe, Influence of anodic oxidation of glassy carbon surface on voltammetric behavior of Nafion (R)-coated glassy carbon electrodes, Electrochim. Acta 46 (2001) 3381.
[22] M.J. Bleda-Martinez, D. Lozano-Castello, E. Morallon, D. Cazorla-Amoros, A. Linares-Solano, Chemical and electrochemical characterization of porous carbon materials, Carbon 44 (2006) 2642.
[23] A. Kuznetsova, I. Popova, J.T. Yates, M.J. Bronikowski, C.B. Huffman, J. Liu, R.E. Smalley, H.H. Hwu, J.G.G. Chen, Oxygen-containing functional groups on single-wall carbon nanotubes: NEXAFS and vibrational spectroscopic studies, J. Am. Chem. Soc. 123 (2001) 10699–10704.
[24] A. Chou, T. Bocking, N.K. Singh, J.J. Gooding, Demonstration of the importance of oxygenated species at the ends of carbon nanotubes for their favourable electrochemical properties, Chem. Commun. 7 (2005) 842.
[25] S. Shiraishi, H. Kurihara, K. Okabe, D. Hulicova, A. Oya, Electric double layer capacitance of highly pure single-walled carbon nanotubes (HiPco (TM) Buckytubes (TM)) in propylene carbonate electrolytes, Electrochem. Commun. 4 (2002) 593.
[26] T. Inoue, S. Mori, S. Kawasaki, Electric Double Layer Capacitance of Graphene-Like Materials Derived from Single-Walled Carbon Nanotubes, Jpn. J. Appl. Phys. 50 (2011) 01AF07.
[27] M.H. Ervin, B.S. Miller, B. Hanrahan, B. Mailly, T. Palacios, A comparison of single-wall carbon nanotube electrochemical capacitor electrode fabrication methods, Electrochim. Acta 65 (2012) 37.
[28] J. Li, A. Cassell, L. Delzeit, J. Han, M. Meyyappan, Novel three-dimensional electrodes: Electrochemical properties of carbon nanotube ensembles, J. Phys. Chem. B 106 (2002) 9299.
[29] R.S. Nicholson, Theory and application of cyclic voltammetry for measurement of electrode reaction kinetics, Anal. Chem. 37 (1965) 135.
[30] E. Mahé, D. Devilliers, Ch. Comninellis, Electrochemical reactivity at graphitic micro-domains on polycrystalline boron doped diamond thin-films electrodes, Electrochim. Acta 50 (2005) 2263.
[31] C.G. Zoski, Handbook of Electrochemistry, first ed., Elsevier, Amsterdam, 2007.
[32] A.M. Bond, E.A. McLennan, R.S. Stojanovic, F.G. Thomas, Assessment of conditions under which the oxidation of ferrocene can be used as standard voltammetric reference process in aqueous-media, Anal. Chem. 59 (1987)2853.
[33] S. Ounnunkad, A.I. Minett, M.D. Imisides, N.W. Duffy, B.D. Fleming, Ch.-Y. Lee, A.M. Bond, G.G. Wallace, Comparison of the electrochemical behaviour of buckypaper and polymer-intercalated buckypaper electrodes, J. Electroanal. Chem. 652 (2011) 52.
[34] C. Sanchís, H.J. Salavagione, E. Morallón, Ferrocenium strong adsorption on sulfonated polyaniline modified electrodes, J. Electroanal. Chem. 618 (2008) 67.
[35] R.H. Wopschall, I. Shain, Effects of adsorption of electroactive species in stationary electrode polarography, Anal. Chem. 39 (1967) 1514.
[36] X. Zhuang, D. Wang, Y. Lin, L. Yang, P. Yu, W. Jiang, L. Mao, Strong Interaction between Imidazolium-Based Polycationic Polymer and Ferricyanide: Toward Redox Potential Regulation for Selective In Vivo Electrochemical Measurements, Anal. Chem. 84 (2012) 1900.
[37] M.S. Dresselhaus, G. Dresselhaus, R. Saito, A. Jorio, Raman spectroscopy of carbon nanotubes, Phys. Reports 409 (2005) 47.
[38] A. Jorio, R. Saito, J.H. Hafner, C.M. Lieber, M. Hunter, T. McClure, G. Dresselhaus, M.S. Dresselhaus, Structural (n, m) determination of isolated single-wall carbon nanotubes by resonant Raman scattering, Phys. Rev. Lett 86 (2001)1118.
[39] M.D. Ganji, M. Hesami, M. Shokry, S. Mahmoudi, Interaction between methanol and single-walled carbon nanotubes: Density functional theory study, Physica B 406 (2011) 1295.
[40] K. Seo, K.A. Park, C. Kim, S. Han, B. Kim, Y.H. Lee, Chirality- and diameter-dependent reactivity of NO2 on carbon nanotube walls, J. Am. Chem. Soc. 127 (2005) 15724.
[41] M. Rajarajeswari, K. Iyakutti, Y. Kawazoe, Effect of chirality and curvature of single-walled carbon nanotubes on the adsorption of uracil, Phys. Status Solidi B 248 (2011) 1431.
[42] P. Chen, M.A. Fryling, R.L. McCreery, Electron-transfer kinetics at modified carbon electrode surfaces- the role of specific surface sites, Anal. Chem. 67 (1995) 3115.
[43] P. Chen, R.L. McCreery, Control of electron transfer kinetics at glassy carbon electrodes by specific surface modification, Anal. Chem. 68 (1996) 3958.
[44] S.H. DuVall, R.L. McCreery, Control of catechol and hydroquinone electron-transfer kinetics on native and modified glassy carbon electrodes, Anal. Chem. 71 (1999) 4594.
[45] S.H. DuVall, R.L. McCreery, Self-catalysis by catechols and quinones during heterogeneous electron transfer at carbon electrodes, J. Am. Chem. Soc. 122 (2000) 6759.
[46] M.R. Deakin, P.M. Kovach, K.J. Stutts, R.M. Wightman, Heterogeneous mechanisms of the oxidation of catechols and ascorbic acid at carbon electrodes, Anal. Chem. 58 (1986) 1474.
[47] A.J. Swallow, in: B.L. Trumpower (Ed.), Function of Quinones in Energy Conserving Systems, Academic Press, New York, 1982, p. 66, Chapter 3.
[48] J.Q. Chambers, in: S. Patai, Z. Rappaport (Eds.), The Chemistry of Quinonoid Compounds;, Vol. II, Wiley and Sons, New York, 1988, p. 719.
[49] A. Barbafina, F. Elisei, L. Latterini, F. Milano, A. Agostiano, M. Trotta, Photophysical properties of quinones and their interaction with the photosynthetic reaction centre, Photochem. Photobiol. Sci. 7 (2008) 973.
[50] C. Costentin, Electrochemical approach to the mechanistic study of proton-coupled electron transfer, Chem. Rev. 108 (2008) 2145–2179.
[51] G.E. Cabanis, A.A. Diamantis, W.R. Murphy Jr., R.W. Linton, T.J. Meyer, Electrocatalysis of proton-coupled electron-transfer reactions at glassy-carbon electrodes, J. Am. Chem. Soc. 107 (1985) 1845.
[52] M.H.V. Huynh, T.J. Meyer, P.S. White, Proton-coupled electron transfer from nitrogen. A N-H/N-D kinetic isotope effect of 41.4, J. Am. Chem. Soc. 121 (1999) 4530.